Journal Pre-proof

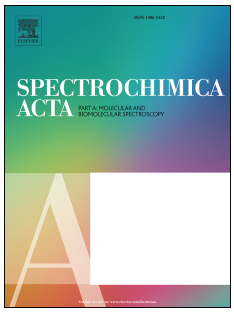

Selection and characterization of DNA aptamers for constructing colorimetric biosensor for detection of PBP2a

Yaofang Fan, Mengyu Cui, Yanming Liu, Minli Jin, Huimin Zhao

PII: S1386-1425(19)31125-4

DOI: https://doi.org/10.1016/j.saa.2019.117735

Reference: SAA 117735

To appear in: *Spectrochimica Acta Part A: Molecular and Biomolecular Spectroscopy*

Received Date: 12 August 2019

Revised Date: 21 October 2019

Accepted Date: 30 October 2019

Please cite this article as: Y. Fan, M. Cui, Y. Liu, M. Jin, H. Zhao, Selection and characterization of DNA aptamers for constructing colorimetric biosensor for detection of PBP2a, *Spectrochimica Acta Part A: Molecular and Biomolecular Spectroscopy* (2019), doi: https://doi.org/10.1016/j.saa.2019.117735.

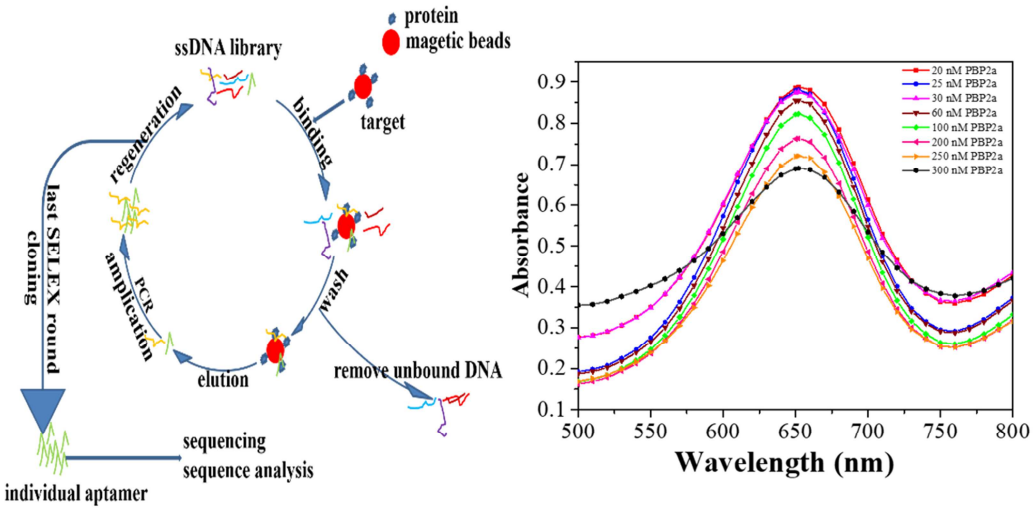

Selection and characterization of DNA aptamers for constructing colorimetric biosensor for detection of PBP2a

Yaofang Fan[1], Mengyu Cui[1], Yanming Liu[1], Minli Jin[2], Huimin Zhao*[1]

1 Key Laboratory of Industrial Ecology and Environmental Engineering (Ministry of Education, China), School of Environmental Science and Technology, Dalian University of Technology, Dalian 116024, China;

2 Department of Immunology, College of Basic Medical Science, Dalian Medical University, Lvshun South Road, Dalian, Liaoning 116044, China

Corresponding e-mail: zhaohuim@dlut.edu.cn

Abstract

Rapid and accurate diagnosis of methicillin-resistant staphylococcus aureus (MRSA) is vital for patient treatment, control of infection and monitoring epidemiology. Penicillin binding proteins (PBP2a), as an important marker protein of MRSA, has been proposed as the screening test target for tolerant bacteria of MRSA. However, current technologies based on PBP2a activity or PBP2a immunoassays were suboptimal specificity and sensitivity. In this report, the selection and characterization of DNA aptamers that binds to PBP2a was described. The DNA aptamer is with high affinity and selectivity to binding with PBP2a. Furthermore, utilizing the switched mimicking peroxidase for gold nanoparticles loaded graphene oxide (GO/Au) nanomaterials based on the effect between GO/Au and DNA, a powerful strategy was set out for designing aptamer-based colorimetric biosensor for detection of PBP2a. In this strategy, the employment of biosensor based on GO/Au and PBP2a aptamer greatly improved the detection sensitivity and selectivity with limit of detection as low as 20 nM. Accordingly, the reversible nanozyme inhibition/activation approach may be universally applicable for the biomedical diagnosis.

Keywords: *PBP2a; aptamer; colorimetric; biosensor; graphene*

Introduction

For decades, a large public hospital healthcare associated with infections resulting from the rapid emergence of antimicrobial resistance. MRSA has been identified as typical antimicrobial since firstly reported in 1959, evidence of penicillin-resistance[1, 2]. More recently, several epidemics of community effect associated MRSA have occurred in healthy populations[3-5]. Universally, MRSA causes varied infections including the hand, skin, mucosal membranes and soft tissue infections[6, 7]. Thereby signifying that achieving a rapid and timely diagnosis is highly desirable to reduce the negative outcomes of MRSA, so that hospital or out-hospital spread of these infections can be effectively controlled and associated risk will decrease.

MRSA acquired resistance to methicillin resistant via *mecA* gene encodes altered PBP2a resulting in low affinity for β-lactam. PBP2a can resist to all β-lactam antibiotics. Alternatively, significant efforts, such as PCR, phenotypic tests and enzyme-linked immunosorbent assay (ELISA), have been directed for detecting PBP2a due to their high expression by most MRSA. However, PCR technology is very time-consuming and labor intensive, also depends on well-defined colony morphology[8-11]. Culture condition including the osmolarity of the medium and temperature may vary phenotypic expression of resistance[12]. Though immunological method has achieved for sensitive detection of MRSA, time-consumption and costly and highly enzyme-dependent make it impractical for clinical diagnosis[13, 14]. Though the development of biosensor offered great opportunity for creative highly sensitive and fast response time for PBP2a detection, the expensive price and poor stability required for antigen still impedes practical application. Aptamers are single-strands nucleic acids (DNA or RNA) which own particular spatial structure with high affinity and specificity to targets in a manner analogous to function of antibodies[15-17]. The unique properties of nucleic acids endow aptamers with lots of relative advantages to antibodies, including non-immune, low-cost, fast time preparation, and thermal stability, resulting widely applied in

various detection applications[18]. Aptamers can be obtained via an exponential enrichment technique known as systematic evolution of ligands by exponential enrichment (SELEX)[19-22].

During the recent years, graphene-based nanomaterials such as graphene oxidase (GO) or graphene oxidase compose, have come out as promising nanomaterials for biosensor due to its excellent electronic and optical properties, good endocytosis and biocompatibility[23-26]. In particular, aptamers can conjugate with graphene via electronic and π-π stacking interaction between graphene surface and nucleotide base, which has successfully been used as detection platform, including electrochemical sensors[27, 28], fluorescent sensors[29-31] and colorimetric sensors[32, 33]. Colorimetric biosensors have attracted great interest due to noncovalent functionalization and unlabeled aptamers[34, 35]. Moreover, our group has reported that the peroxidase-like activity of GO/Au can be differently influenced by single-stranded DNA (ssDNA). In particularly, take GO/Au as nanozyme enhanced peroxidase-like activity has been regarded as a promising method to achieve aptamer label-free detection[36]. However, the lack of research on aptamer for selection of PBP2a impedes the graphene/Au-aptamer based colorimetric detection platform construction.

In this work, the process was reported of selection and characterization of PBP2a aptamers with high affinity and selectivity. Moreover, an engineering of a colorimetric biosensor for PBP2a detection was employed based on the switchable peroxidase-like activity of GO/Au nanomaterials and PBP2a aptamer. The biosensor shows high sensitivity and specificity to targets and achieved detection limit as low as 20 nM.

Materials and method

Chemicals and reagents

The nucleic acids library was obtained from LLC X-aptamer selection Kit (AM biotechnologies, America). PBP2a (His-tagged) was purchased from Sangon (Shanghai, China). Pfu DNA polymerase, 5×TBE, Ammonium persulfate, N, N, N', N'-Tetramethylethylenediamine, 2×TBE-Urea Sample Buffer TBE-Urea Sample Buffer, dNTP buffer, Acryl/Bis 40% solution and Ammonium were obtained from Sangon (Shanghai, China). All other reagents used in this paper were analytic degree without any purification in use. Ultrapure water was obtained via a Millipore water purification system (Laikie Instrument Co., Ltd., Shanghai, China). Gel electrophoresis was performed by mini camera-obscura UV system GL-200.

Characterization

Transmission electron microscopy (TEM) images were gained from high-magnification TEM (FEI Tecnai G2 F30 S-Twin). Jasco V-550 spectrometer was employed for ultraviolet-visible (UV-vis) absorption spectra. Polymerase chain reaction (PCR) was obtained from PCR instrument (T100, bio-rad, Singapore). Table-top and high-speed refrigerated centrifuge was used for nucleic acid recycling.

In vitro selection of aptamers

The protocols of aptamer selection for PBP2a were performed according to LLC X-aptamer selection Kit. B. Briefly, selection buffer preparation, two buffers (selection buffer A (1×PBS pH 7.4, 0.05% tween 20, 1 mM $MgCl_2$), selection buffer B (1×PBS pH 7.4, 0.05% tween 20, 1mM $MgCl_2$, 0.2% BSA)). Preparation of library, resuspend the library with buffer A, leaving all beads in the tube, as well as 95 °C for 5 minutes. Protein preparation, utilizing His-tagged PBP2a hatching with Biotin.

Negative selective. Coupling of target protein on magnetic particles. Positive selection. Cleavage putative aptamers. Spinning column buffer exchange. Secondary pulls down selection. PCR and gel analysis. Starting Additional pool PCR. Next generating sequence. Data analysis and candidate X-Aptamer synthesis by AM Biotechnologies.

Identification of high-affinity aptamer and specificity for PBP2a

Q-PCR was employed for evaluating the binding characteristic of several aptamers. Briefly, the protein was labeled with biotin, and biotin-labeled proteins were purified. Quantitative detection of biotin based on UV-vis. Calculating the number of biotin moles per mole of protein.

The selectivity of aptamer was performed by electrophoretic mobility shift assays (EMSA). Binding analyses were conducted in 200 μL of 1×binding buffer containing 3 nM PBP2a aptamer and 30 nM PBP2a, 1000 nM proteinase K, 1000 nM GOx and 1000 nM BSA. After incubation for 60 min, the reaction mixtures were spiked with 2×TBE-Urea sample buffer, and subsequently loaded into the wells of the non-denaturing polyacrylamide gel (8%) at room temperature. Visualization of DNA bands was performed by mini camera-obscura UV system GL-200.

Preparation of rGO/Au

Graphene oxidase was synthesized according to an improved published route of Hummers' method with additional of $KMnO_4$. The rGO/Au was prepared via our previous reports. Briefly, 2.5 mL GO (0.5 mg/mL), 1.0 mL $HAuCl_3 \cdot 3H_2O$ (10 mM), 1.1 mL NaOH (0.1 M) and 20.4 mL ultrapure water were mixed under vigorous stirring for 0.5 h. The mixture was transferred into a Teflon-lined autoclave for 10 h at 180 °C. The product was centrifuged and washed by ultrapure water several times.

Detection of PBP2a and selectivity

100 μL rGO/Au (0.05 mg/mL), 90 μL ultrapure water were mixed with 100 μL TMB (10 mM) and 100 μL H_2O_2 (10 mM) at acetate buffer (pH = 4) for 30 min in room temperature. For detecting PBP2a, 10 μL aptamer (5 μM) in buffer, 30 μL different concentrations of PBP2a and 100 μL rGO/Au (0.05 mg/mL) were incubated at room temperature for 2 h, followed by 100 μL TMB (10 mM) and 100 μL H_2O_2 (10 mM) at acetate buffer (pH = 4). After being incubated for 30 min at room temperature, the absorbance of these solutions in a cell was measured with 652 nm excitation. For analyzing aptasensor on selective properties of PBP2a, 10 μL aptamer (5 μM) in buffer, 30 μL other three protein (1000 nM) and 100 μL rGO/Au (0.05 mg/mL) were incubated at room temperature for 2 h, followed by 100 μL TMB (10 mM) and 100 μL H_2O_2 (10 mM) at acetate buffer (pH = 4). After being incubated for 30 min at room temperature, the absorbance of these solutions in a cell was measured with 652 nm excitation.

Results and discussion

The selection strategy was illustrated in Scheme 1. A special DNA library in the selection process was used, which contained a central 13 baes pairs (bp) nucleotides fixed sequence at 5 flank, 5 bp nucleotides fixed sequence at 3 flank and 42 bp random region at central. Notably, some bases were modified nucleotides indole-dU, phenol-dU and amine-dU. PBP2a (C-terminal $(His)_6$-tag) was hatching with Biotin. The initial DNA library (typically 10^8 members) was mixed with PBP2a-coated magnetic particles. Some aptamers were then released from beads and followed by a secondary pull down to remove false-positive aptamers. Subsequently, the true aptamers were identified via next-generation methods by Sangon Biotech. Data analysis and candidate aptamers synthesis was supplied by AM Biotechnologies.

Scheme 1

After the PBP2a aptamer screening process, the amplified and extracted DNAs produced were examined by gel electrophoresis (Fig. 1). The length of DNAs was from 75 bp to 100 bp. The result of gel electrophoresis shows that the target PBP2a specific DNA aptamer was successfully amplified and extracted by the system. The concentration of the aptamers is enough for the high through-put sequencing.

Fig. 1

After data analysis and aptamer synthesis, the top 8 highest multiplicity sequences for PBP2a were investigated in Table 1. W, Y and X represents modified nucleotides indole-dU, phenol-dU and amine-dU, respectively. The sequence was chosen for its ability to bind with PBP2a via Q-PCR for testing affinity.

Table 1

The equilibrium dissociation constants (K_d) was calculated in the low concentration range. The lowest K_d value of was obtained for S1 and S3. The K_d values of the two aptamers were 30 nM and 15 nM, respectively. As known that the lower of the K_d value represents the higher of the affinity, confirming that the affinity of S3 to the PBP2a was better than that of SA. To explore the structure difference among the aptamers, the theoretical secondary structures was estimated by using the Mfold program based on a dynamic program of lowest free energy (Fig. 2). Typically, different stem-loop motifs were found in secondary structure, which has been frequently reported in many other previously RNA or DNA aptamers. The stem-loop motifs may be the mainly functionalized domain for binding with PBP2a.

Fig. 2

As known that some nucleoids usually have affinity to several targets. The highest aptamer, S3, was then chosen for studying functional binding specificity to PBP2a via EMSA. Except for PBP2a, no obvious band can be observed when using other proteins such as Proteinase K, GOx and BSA (Fig. 3), indicating that S3 showed excellent affinity and specificity to PBP2a.

Fig. 3

The S3 aptamer was then used for constructing a colorimetric-based biosensor to detect PBP2a. Biosensors via colorimetric method has attracted numerous attentions in designing of multifarious biosensors owning to its sensitivity and simplicity. Our group has demonstrated that the peroxidase activity of graphene can be regulated by ssDNA due to the multiplexed interaction between ssDNA and graphene, which have been successfully employed for establishing colorimetric sensor platform. In the presence of targets, aptamers will release from GO/Au to the targets leading to variation of UV-vis absorbance due to the change of catalytic activity of GO/Au. In spite of the general utility of the approach, the construction of colorimetric aptasensor based on the GO/Au nanomaterials still remains challenge due to significant conformational change of aptamers in the presence of targets. Therefore, to overcome the problem, PBP2a aptamer coupled with GO/Au was employed for constructing biosensor for PBP2a detection. The micromorphology of prepared GO/Au was characterized by TEM (Fig. 4a). The TEM images showed the Au nanoparticles well dispersed on the surface of the graphene surface. HRTEM images exhibit that the lattice fringes of Au nanoparticles with an interplane distance of 0.233 nm (Fig. 4b) refer to the (111) plane of Au particles with the previous reports. The results above indicated that the GO hybrids with Au nanoparticles were successfully synthesized.

Fig. 4

Based on the successful fabrication of GO/Au, the peroxidase-like activity was evaluated by oxidation of TMB in the presence of H_2O_2. Fig. 5 shows that the prepared GO/Au possess peroxidase activity for catalyzing TMB producing blue color in the presence H_2O_2 with an absorbance maximum at 652 nm. In contrast, there is no absorbance change under the same concentration of H_2O_2 alone. In order to validate the effect of PBP2a adsorption for peroxidase activity of GO/Au, an absorbance test was also evaluated. As shown in Fig. 5, the absorbance maximum at 652 nm of GO/Au with PBP2a aptamer significantly enhanced compared to GO/Au alone, revealing that the PBP2a aptamer can up-regulate the peroxidase-like activity of GO/Au. The phenomenon may be attributed to both aromatic stacking and electrostatic interaction with the substrate TMB[37]. It lays as foundation for detection of PBP2a used for the interaction between GO/Au and PBP2a aptamer.

Fig. 5

Aforementioned that sensitive and selective diagnostic approaches for PBP2a detection are urgently need for early and accurate detection. On the basis of PBP2a aptamer effect on the peroxidase like activity of GO/Au, a strategy is investigated by monitoring the absorbance change of substrate TMB in the presence of different concentration of PBP2a. As shown in Fig. 6a, in the presence of PBP2a, the absorbance maximum at 652 nm reduced gradually. The absorbance of PBP2a at 652 nm linearly depends on the concentration of PBP2a from 20 nM to 300 nM with a regression coefficient of 0.999 (Fig. 6b). The result reveals that a colorimetric aptasensor platform based on GO/Au as nanozyme was successfully established for PBP2a detection. The results above indicated that the proposed assay presents a

sensitive aptasensor platform for PBP2a detection.

Fig. 6

Escherichia coli (E.coli) transfected with *mec A* as model was investigated to the practical application of this biosensor for the real samples. After breakdown of the inducible expression of bacteria (1.9×10^9 cfu/mL, 3L), cell lysis solution was collected in total of 500 μL. The solution was diluted 10^0, 10^1 and 10^2 fold. With the addition of various concentration of cell lysis solution mixture into the reaction system of GO/Au and aptamer without PBP2a, the absorbance of final solution was detected by UV-vis absorption spectra at 652 nm. As shown in Figure 7b, with the concentration of cell lysis solution increasing, the absorbance was decreased gradually at 652 nm. The results suggest that the feasibility of this method is for the detection of real samples. For analyzing aptasensor on selective properties of PBP2a, 30 μL of 300 nM PBP2a, 1000 nM proteinase K, 1000 nM GOx, and 1000 nM BSA was added to the reaction system under the same detected system, respectively. Please note, the concentration of other three proteins was 3 times higher than that of PBP2a. The absorbance of these solutions in a cell was measured with 652 nm excitation (As shown in Figure 7a). Since the absorbance of three other proteins is higher than that of PBP2a at 652 nm, considering the differences of their concentrations, it is reasonable to think that this method possessed good selectivity for PBP2a detection.

Fig. 7

Conclusion

To summarize, the aptamer of PBP2a was successfully selected with high affinity and specificity based on SELEX technology. The high specificity of aptamer and PBP2a interaction provided the outstanding selectivity for PBP2a detection. Furthermore, a

colorimetric reliable aptasensor strategy for highly sensitive and selective detection of PBP2a was proposed on the basis of the peroxidase-like activity of GO/Au mimics. The sensitivity of the aptasensor to PBP2a is significant with detection range from 20 nM to 300 nM. The proposed aptasensor potentially offer a novel approach for the detection of PBP2a. Furthermore, this technique possesses great potential for using in the diagnosis of diseases associated with MRSA.

Acknowledgement

This work was supported by the National Nature Science Foundation of China (No. 21477012).

Reference

1. A. B. Bandara, Z. Zuo, S. Ramachandran, A. Ritter, J. R. Heflin and T. J. Inzana, Detection of methicillin-resistant staphylococci by biosensor assay consisting of nanoscale films on optical fiber long-period gratings, Biosens. Bioelectron. 70 (2015) 433-440.
2. C. P. Harkins, B. Pichon, M. Doumith, J. Parkhill, H. Westh, A.Tomasz, H. de Lencastre, S. D. Bentley, A. M. Kearns and M. T. G. Holden, Methicillin-resistant Staphylococcus aureus emerged long before the introduction of methicillin into clinical practice, Genome biol. 18.1 (2017) 130.
3. B. Ballhausen, A. Kriegeskorte, S. van Alen, P. Jung, R. Köck, G. Peters, M. Bischoff, K. Becker, The pathogenicity and host adaptation of livestock-associated MRSA CC398, Vet. Microbiol. 200 (2017) 39-45.
4. D. Bencardino, L. A. Vitali, Staphylococcus aureus carriage among food handlers in a pasta company: pattern of virulence and resistance to linezolid, Food control. 96 (2019) 351-356.
5. W. C. Hung, T. W. Wan, Y. C. Kuo, T. Yamamoto, J. C. Tsai, Y. T. Lin, P. R. Hsush and L.J. Teng, Molecular evolutionary pathways toward two successful community-associated but multidrug-resistant ST59 methicillin-resistant Staphylococcus aureus lineages in Taiwan: dynamic modes of mobile genetic element salvages, PloS one 11.9 (2016) e0162526.
6. N. V. Enwuru, S. A. Adesida, C. A. Enwuru, B. Ghebremedhin, U.

E. Mendie and A. O. Coker, Genetics of bi-component leukocidin and drug resistance in nasal and clinical Staphylococcus aureus in Lagos, Nigeria, Microb pathogenesis 115 (2018) 1-7.

7. C.D. Santos-Junior, A. Verissimo, J. Costa, The recombination dynamics of Staphylococcus aureus inferred from spA gene, BMC microbiol. 16.1 (2016) 143.
8. M. A. Akindolire, O. O. Babalola, and C. N. Ateba, Detection of Antibiotic Resistant Staphylococcus aureus from Milk: A Public Health Implication, Inter J Env Res Pub Heal. 12.9 (2015) 10254-10275.
9. F. Alipour, M. Ahmadi and S. Javadi, Evaluation of different methods to detect methicillin resistance in Staphylococcus aureus (MRSA), J INFECT PUBLIC HEAL, 7.3 (2014) 186-191.
10. J. A. Delport, I. Mohorovic, S. Burn, J. K. McCormick, D. Schaus, R. Lannigan and M. John, Rapid detection of meticillin-resistant Staphylococcus aureus bacteraemia using combined three-hour short-incubation matrix-assisted laser desorption/ionization time-of-flight MS identification and Alere Culture Colony PBP2a detection test, J Med Microbiol. 65.7 (2016) 626-631.
11. B. Mantion, L. Cavalié, M.-F. Prère, Evaluation of an immunochromatographic assay for detection of PBP2a on non-Staphylococcus aureus clinical isolates, J Microbiol Meth. 112 (2015) 46-48.
12. J. Tasse, C. Dupieux, J. Caillon, P. Lanotte, B. Lamy, N. Aissa, P. Bemer, L. Mereghetti, A-L. Michon, A. Lozniewski, M. Bes, S. T. Assant, F. Laurent, Rapid bench identification of methicillin-sensitive and methicillin-resistant Staphylococcus aureus: A multicenter comparative evaluation of Alere PBP2a Culture Colony Test (Alere) Versus Slidex MRSA detection (bioMerieux), Diagn Micr Infec Dis. 85.4 (2016) 419-421.
13. M. Chung, C. K. Kim, T. Conceição, M. Aires-De-Sousa, H. De Lencastre, A. Tomasz, Heterogeneous oxacillin-resistant phenotypes and production of PBP2A by oxacillin-susceptible/mecA-positive MRSA strains from Africa, J Infect Chemother. 71.10 (2016) 2804-2809.
14. A.A.S. Gill, S. Singh, N. Thapliyal, R. Karpoormath, Nanomaterial-based optical and electrochemical techniques for detection of methicillin-resistant Staphylococcus aureus: a review, Microchimica Acta 186.2 (2019) 114.
15. L. Chen, W. He, H. Jiang, L. Wu, W. Xiong, B. Li, Z. Zhou and Y. Qian, In vivo SELEX of bone targeting aptamer in prostate cancer bone metastasis model，Int J Nanomed 14 (2019) 149.

16. D. Cheng, M. Yu, F. Fu, W. Han, G. Li, J. Xie, Y. Song, M.T. Swihart, E. Song, Dual Recognition Strategy for Specific and Sensitive Detection of Bacteria Using Aptamer-Coated Magnetic Beads and Antibiotic-Capped Gold Nanoclusters, Anal Chem, 88.1 (2016) 820-825.
17. J. Jaeger, F. Groher, J. Stamm, D. Spiehl, J. Braun, E. Dörsam, B. Suess, Characterization and Inkjet Printing of an RNA Aptamer for Paper-Based Biosensing of Ciprofloxacin, Biosensors 9.1 (2019) 7.
18. J. He, J. Wang, N. Zhang, L. Shen, L. Wang, X. Xiao, Y. Wang, T. Bing, X. Liu, S. Li, D. Shangguan, In vitro selection of DNA aptamers recognizing drug-resistant ovarian cancer by cell-SELEX, Talanta, 194 (2019) 437-445.
19. D. Liu, Z. Zhang, Y. Yin, F. Jia, Q. Wu, P. Tian, D. Wang, Development and evaluation of a novel in situ target-capture approach for aptamer selection of human noroviruses, Talanta 193 (2019) 199-205.
20. J. Wang, T. Gao, Y. Luo, Z. Wang, Y. Zhang, Y. Zhang, R. Pei, In Vitro Selection of a DNA Aptamer by Cell-SELEX as a Molecular Probe for Cervical Cancer Recognition and Imaging, J. Mol. Evol. 87.2-3 (2019) 72-82.
21. T. Yoshitomi, F. Wayama, K. Kimura, K. Wakui, H. Furusho, K. Yoshimoto, Screening of DNA Signaling Aptamer from Multiple Candidates Obtained from SELEX with Next-generation Sequencing, Anal. Sci .35.1 (2019) 113-116.
22. Y. Zheng, Y. Zhao, Y. Di, C. Xiu, L. He, S. Liao, D. Li, B. Huang, DNA aptamers from whole-serum SELEX as new diagnostic agents against gastric cancer, RSC advances 9.2 (2019) 950-957.
23. N.A. Hussien, N. Isiklan, and M. Turk, Aptamer-functionalized magnetic graphene oxide nanocarrier for targeted drug delivery of paclitaxel, Mater.Chem.Phys. 211 (2018) 479-488.
24. M. Wu, R. Kempaiah, PJJ. Huang, V. Maheshwari, J. Liu , Adsorption and desorption of DNA on graphene oxide studied by fluorescently labeled oligonucleotides, Langmuir 27.6 (2011) 2731-2738.
25. Y. Song, K. Qu, C. Zhao, J. Ren, X. Qu, Graphene oxide: intrinsic peroxidase catalytic activity and its application to glucose detection, Adv Mater. 22.19 (2010) 2206-2210.
26. H. Sun, Y. Zhou, J. Ren, X. Qu, Carbon Nanozymes: Enzymatic Properties, Catalytic Mechanism, and Applications, Angew. Chem. Int. Ed. 57.30 (2018) 9224-9237.
27. P.K. Pathania, J.K. Saini, S. Vij, R. Tewari, P. Sabherwal, P. Rishi, R. Suri, Aptamer functionalized MoS2-rGO nanocomposite based

biosensor for the detection of Vi antigen, Biosens. Bioelectron. 122 (2018) 121-126.
28. B. Wei, K. Mao, N. Liu, M. Zhang, Z. Yang, Graphene nanocomposites modified electrochemical aptamer sensor for rapid and highly sensitive detection of prostate specific antigen, Biosens. Bioelectron. 121 (2018) 41-46.
29. C. Lu, H. Yang, C. Zhu, X. Chen, G. Chen, A graphene platform for sensing biomolecules. Angew. Chem. Int. Ed. 48.26 (2009) 4785-4787.
30. S. He, B. Song, D. Li, C. Zhu, W. Qi, Y. Wen, L. Wang, S. Song, H. Fang, C. Fan, A Graphene Nanoprobe for Rapid, Sensitive, and Multicolor Fluorescent DNA Analysis, Adv. Funct. Mater.20.3 (2010) 453-459.
31. X. Zhao, Q. Ma, X. Wu, X. Zhu, Graphene oxide-based biosensor for sensitive fluorescence detection of DNA based on exonuclease III-aided signal amplification, Anal. Chim. Acta. 727 (2012): 67-70.
32. Y. Tao, Y. Lin, J. Ren, X. Qu, Self-assembled, functionalized graphene and DNA as a universal platform for colorimetric assays. Biomaterials 34.20 (2013) 4810-4817.
33. J. Thavanathan, N.M. Huang, and K.L. Thong, Colorimetric detection of DNA hybridization based on a dual platform of gold nanoparticles and graphene oxide, Biosens. Bioelectron. 55 (2014) 91-98.
34. F. Sang, X. Zhang, J. Liu, S. Yin, Z. Zhang, A label-free hairpin aptamer probe for colorimetric detection of adenosine triphosphate based on the anti-aggregation of gold nanoparticles. Spectrochim Acta Part A Mol Biomol Spectrosc 217 (2019) 122-127.
35. S. Wu, Q. Yu, C. He, N. Duan, Colorimetric aptasensor for the detection of mercury based on signal intensification by rolling circle amplification. Spectrochim Acta Part A Mol Biomol Spectrosc (2019) 117387.
36. F Yuan, H Zhao, H Zang, F Ye, X.Quan, Three-Dimensional Graphene Supported Bimetallic Nanocomposites with DNA Regulated-Flexibly Switchable Peroxidase-Like Activity. ACS Appl Mater Interfaces, 8.15 (2016) 9855-9864.
37. B. Liu, and J. Liu, Accelerating peroxidase mimicking nanozymes using DNA, Nanoscale 7.33 (2015) 13831-13835.

Figure legends

Scheme 1. In vivo selection of PBP2a aptamers

Figure 1. The extracted and amplified DNAs after the last round were seen by gel electrophoresis. 1: DNA ladders; 2: Control of initial solution; 3: PBP2a; 4: Magnetic beads contrast.

Table 1. Data analysis and aptamer synthesis.

Figure 2. Secondary structures of S1 and S3.

Figure 3. The sequence of PBP2a aptamer incubated with PBP2a, Proteinase K, GOx and BSA.

Figure 4. TEM (a) and HRTEM (b) images of GO/Au.

Figure 5. Peroxidase-like property of different reaction systems.

Figure 6. UV-vis absorption spectra of the GO/Au and aptamer incubated with different concentration of PBP2a (a). Liner relationship between the absorbance value at 652 nm (b) at concentration of 20 nM to 300 nM.

Figure 7. Selectivity analysis of PBP2a detection via colorimetric peroxidase mimetic assay of GO/Au (a). UV-vis absorption spectra of the GO/Au and aptamer incubated with various concentration of cell lysis solution (b).

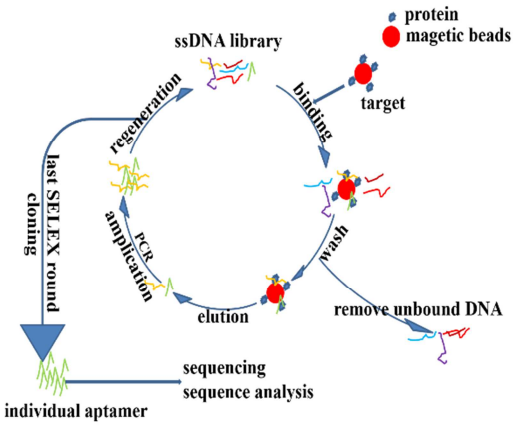

Scheme 1. In vivo selection of PBP2a aptamers

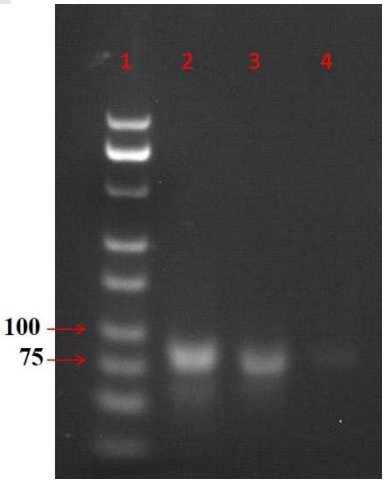

Fig. 1

457 Table 1. Data analysis and aptamer synthesis

Sequence	（5’- 3’）
S1	TTTTTAACACGACAGCCCYGTGGWAGXCGAACCAAWACAC TGTGGGCCCATG
S2	TTTTTAAGCCCACACACGWYCGAAXCACGAACAYCATGCC CGTGGGCCCATG
S3	TTTTTAAGCCCACGAACCYGTGCCXCACGAACTAAWTGCCA GXCGYGCCATG
S4	TTTTTAAGCCCACAAGCCYGTGCWCAXCACAGTGYGTWGA GGTGGGCCCATG
S5	TTTTTAAGCCCACAGGWCYGTGGWGGXCACAGCYCGTCAA GGXCGYGCCATG
S6	TTTTTAAGCCCACAAGGGWYCGAAAGXCGAACAAYGGGCA AGXCGYGCCATG
S7	TTTTTAACACGACXGGWGWYCGGGCAXCGAACGCCACCA GTGTGGGCCCATG
S8	TTTTTAAGCCCACGYGCCYGTGCWGGCCACAGTCCGACAG GGXCGYGCCATG

458

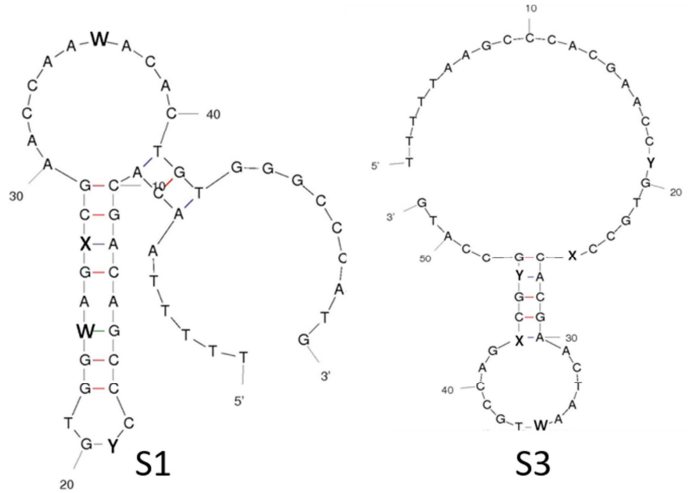

459

460 **Fig. 2**

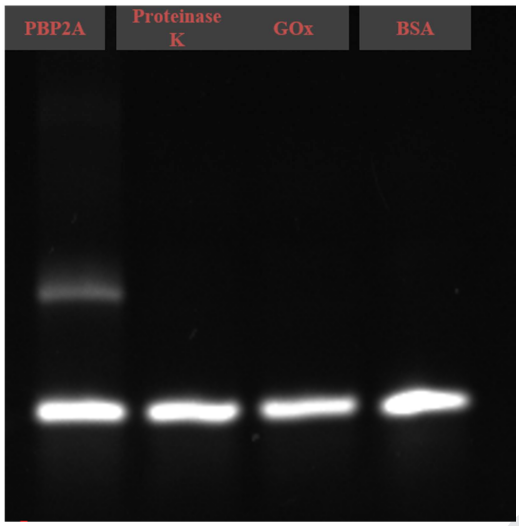

461

462 **Fig. 3**

463

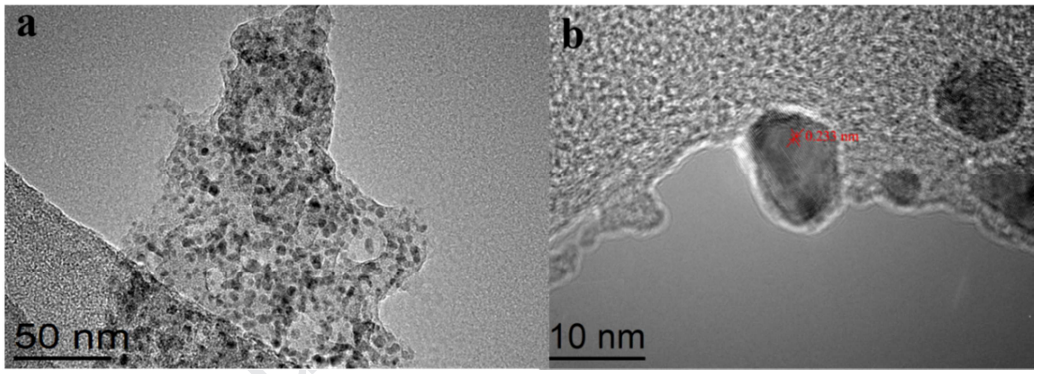

464

465 **Fig. 4**

466

467

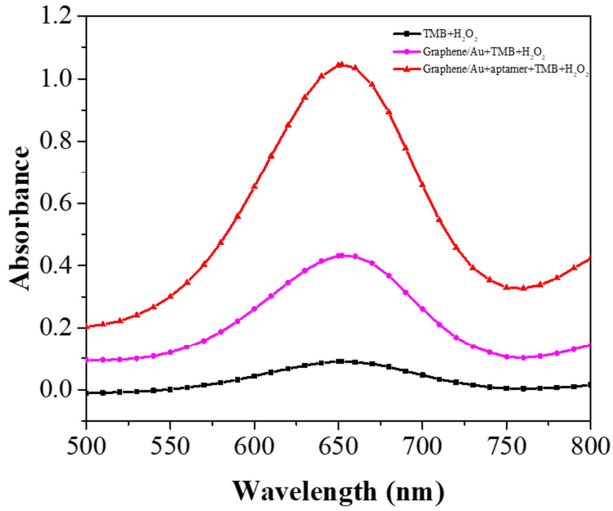

468

469 **Fig. 5**

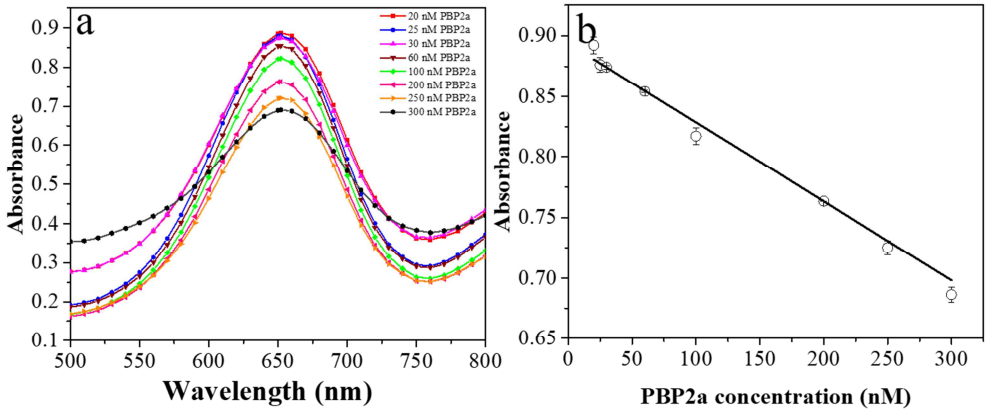
a
20 nM PBP2a
25 nM PBP2a
30 nM PBP2a
60 nM PBP2a
100 nM PBP2a
200 nM PBP2a
250 nM PBP2a
300 nM PBP2a
Absorbance
Wavelength (nm)
b
Absorbance
PBP2a concentration (nM)

Fig. 6

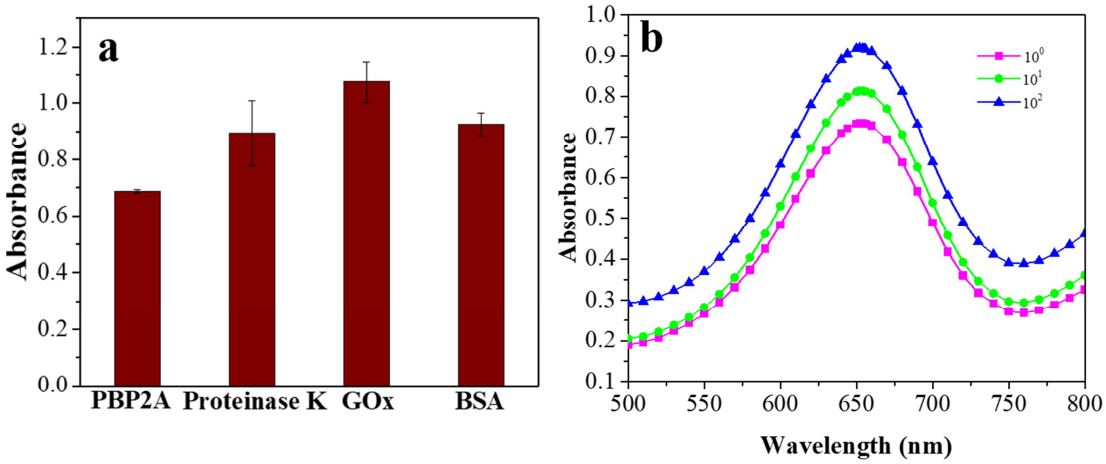
a
Absorbance
PBP2A
Proteinase K
GOx
BSA
b
10^0
10^1
10^2
Absorbance
Wavelength (nm)

Fig. 7

Highlight

1. Aptamers of PBP2a was selected.
2. A colorimetric biosensor based on GO/Au was constructed for detection of PBP2a.